4 Blazars and the AGN Unification Paradigm

• Bl Lac was a prototype AGN for a class of **Bl Lac objects** that exhibited few optical emission lines, contrasting Seyferts, radio galaxies and quasars.

C & O, pp. 1106

∗ The optical and radio continua exhibited strong linear polarization, suggestive of synchrotron radiation. The rapid variability on hour/day timescales again suggested the presence of an SMBH that powers the source. They also exhibit variable X-ray continuum emission.

∗ Much more luminous cousins of the Bl Lacs are the **Optically Violently Variable (OVV) Quasars**, whose spectra may display broad emission lines.

The rapid and dramatic variability led to the term **blazars** collectively describing these two classes.

• A profound change to the blazar paradigm was spawned by the discovery by the **Compton Gamma-Ray Observatory** (CGRO) in 1991–1993 of powerful gamma-ray emission above 100 MeV coming from blazars (e.g. 3C 279) and quasars (e.g. 3C 273).

∗ In a νF_ν plot, the spectra peak in the gamma-rays, indicating that this is where the major portion of the radiative power is, i.e. SMBH energy deposition connects directly to the gamma-rays.

Plot: Broadband Continuum Spectra of Mrk 421

This finding was augmented by the subsequent discovery by the ground-based Atmospheric Čerenkov Telescope **Whipple** of TeV gamma-ray emission by the blazars Mrk 421 and Mrk 501 (Markarian) at $z = 0.033$.

• Flares in blazars can be of extremely short duration, down to minutes simultaneously in X-ray and TeV gamma-rays. This can be accommodated by the shock acceleration paradigm, wherein acceleration rates proceed at the gyrofrequency and are very rapid. It can also be explained by rapid acceleration (with rates scaling with the plasma frequency) associated with **reconnection** of magnetic fields.

Plot: Short Timescale X-ray and TeV Variability in Mrk 421

Multi-wavelength Low-state SED: *Fermi*-LAT Blazar Mrk 421

z=0.033

Abdo et al. (2011)

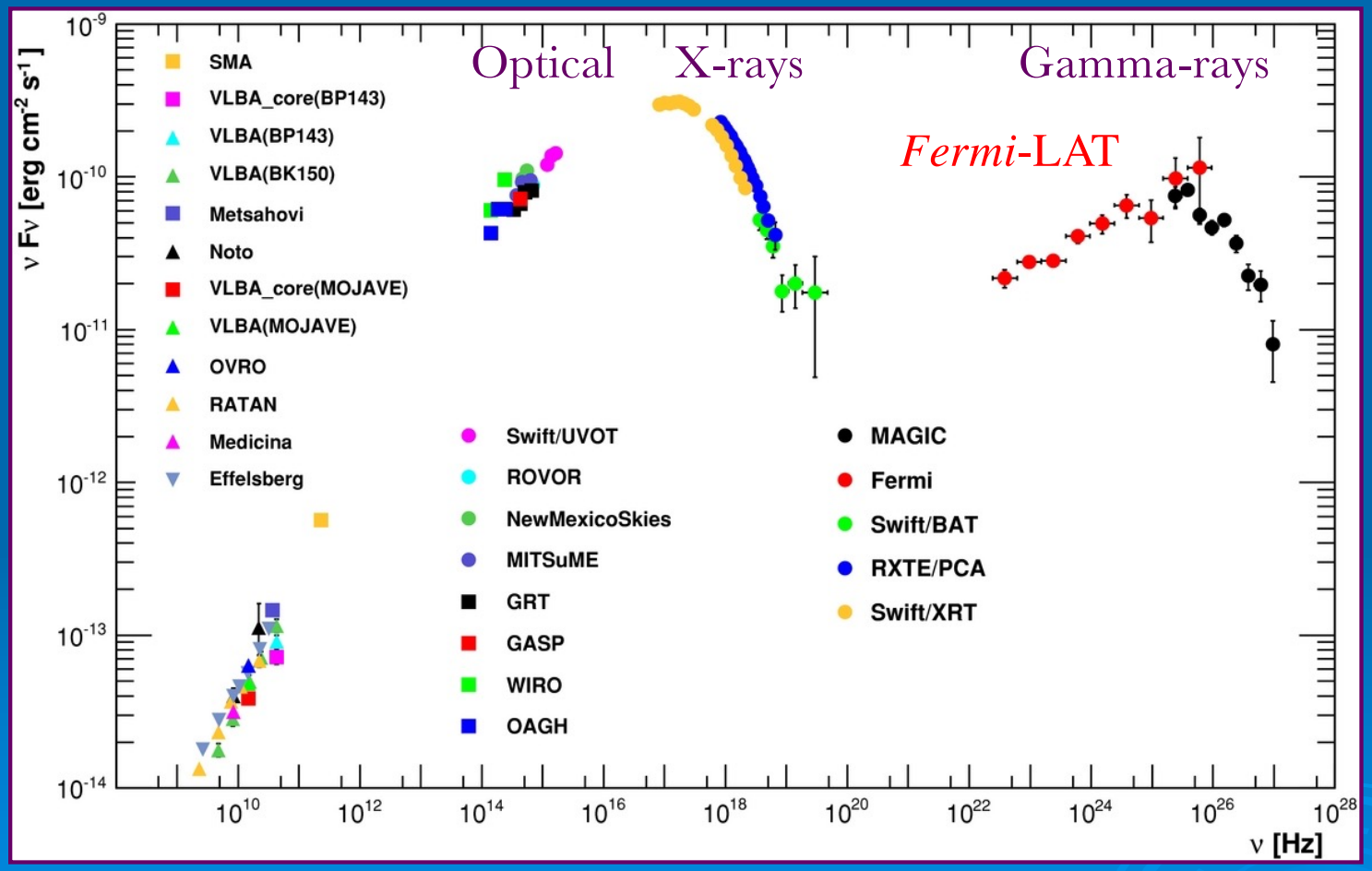

- Spectral energy distribution of Mrk 421 averaged over all the observations taken during the multifrequency campaign from 2009 January 19 (MJD 54850) to 2009 June 1 (MJD 54983). The TeV data from MAGIC were corrected for the absorption in the EBL using the prescription given in Franceschini et al. (2008). Fig. 8 from Abdo et al. (2011, ApJ **736**, 131).

Rapid Variability in Markarian 421

- Fast variability on < 2 hour timescales is seen in UV, X-ray and TeV gamma-rays in the April 1998 flare of Mrk 421 (z=0.033).
  - => compact emission region, < 10-20 AU.
- Takahashi et al. (2000).

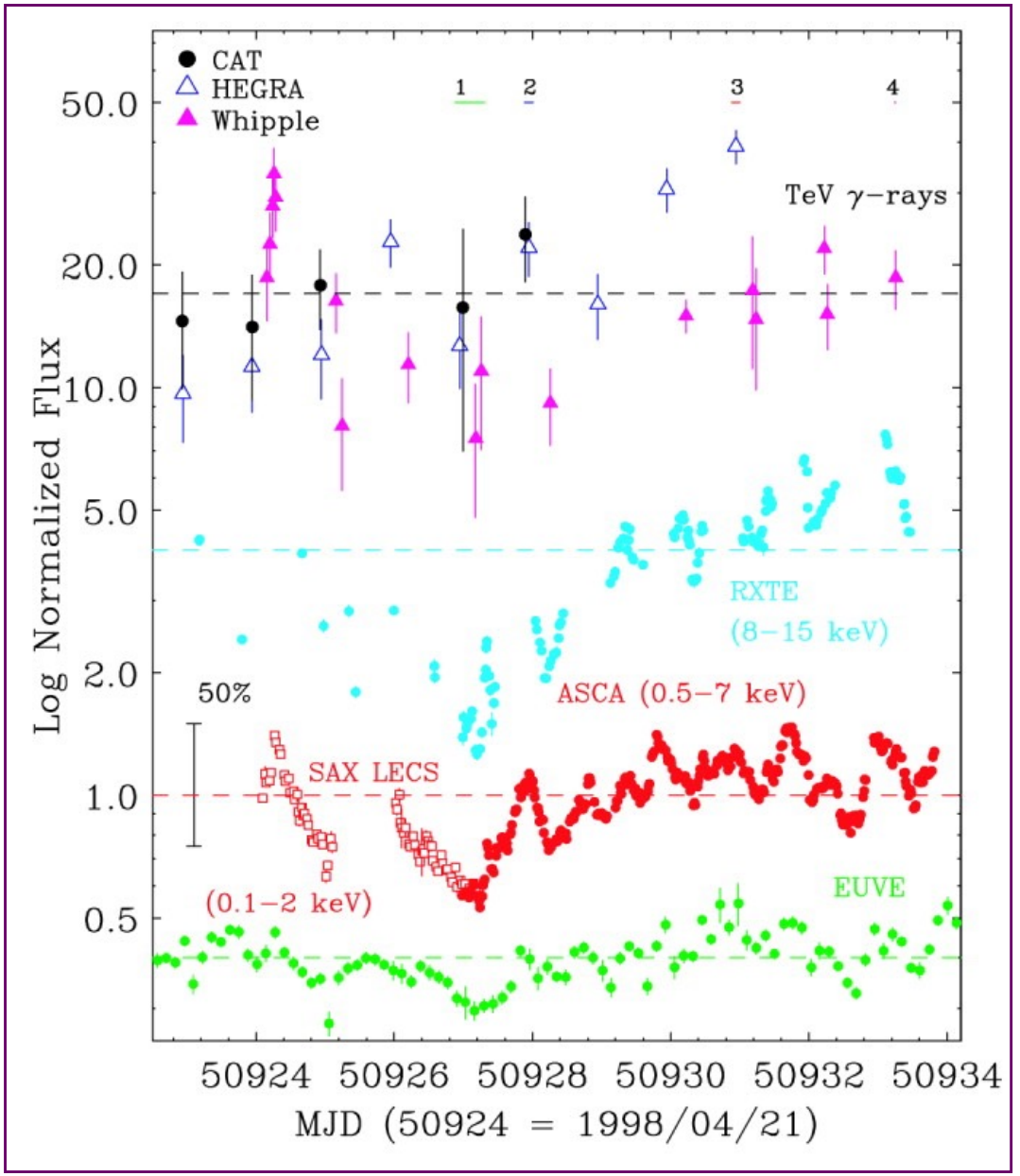

• Blazar emission is thought to originate from relativistic jets like those seen in radio galaxies. The variability in all wavebands in blazars is attributed to changes in the Doppler boosting factor incurred when the jet "wiggles" — small changes an angular perspective lead to *large changes in apparent luminosity* through the impact of the Doppler boosting factor $\mathcal{D}$.

This completes the geometric **AGN Unification Paradigm**, due to Padovani and Urry, with blazars being those AGN that are viewed almost along the jet.

Plot: AGN Geometry for the Unification Paradigm

• While the X-rays are thought to be synchrotron radiation from the most energetic electrons in the jet, the leading model for the gamma-ray components is **synchrotron self-Compton** (off the X-ray continuum) or **inverse Compton** (off the UV bump disk emission) radiation.

∗ A prominent alternative scenario is **hadronic emission** from jets via γp interactions that spawn pions and **neutrinos** as decay products.

∗ The neutrino signal from such models is a key diagnostic that is being probed by major high energy neutrino arrays such as IceCube in Antarctica. In particular, in 2017, IceCube detected a single PeV ν from the blazar TXS 0506+056 in conjunction with a gamma-ray flare detected by *Fermi*-LAT at GeV energies, with a further 13 neutrinos in archival data. Icecube has since detected νs from the Seyfert II galaxy NGC 1068 in the 1-10 TeV band. There is also the very recent discovery by the KM3NeT array in the Mediterranean of a possible 200 PeV neutrino.

Plot: IceCube Observations of Neutrinos from AGN

• The blazar phenomenon has helped spawn a discipline of **multiwavelength** observations of AGNs, dating from the mid-1990s, where sources are monitored in campaigns to assess variability and associated leads/lags simultaneously in radio, optical, X-ray and gamma-ray wavebands. The neutrino detections have extended this to frame a **multi-messenger** emphasis.

• TeV gamma-ray emission is partially attenuated at moderate z due to pair production interactions $\gamma\gamma \to e^+e^-$ with the infrared background radiation from dust in galaxies. Blazars such as Mrk 421 and Mrk 501 can be used as probes of the IR background, once their intrinsic source spectra are understood. Currently they can bound the IR field.

Generic AGN Geometry

Blazars

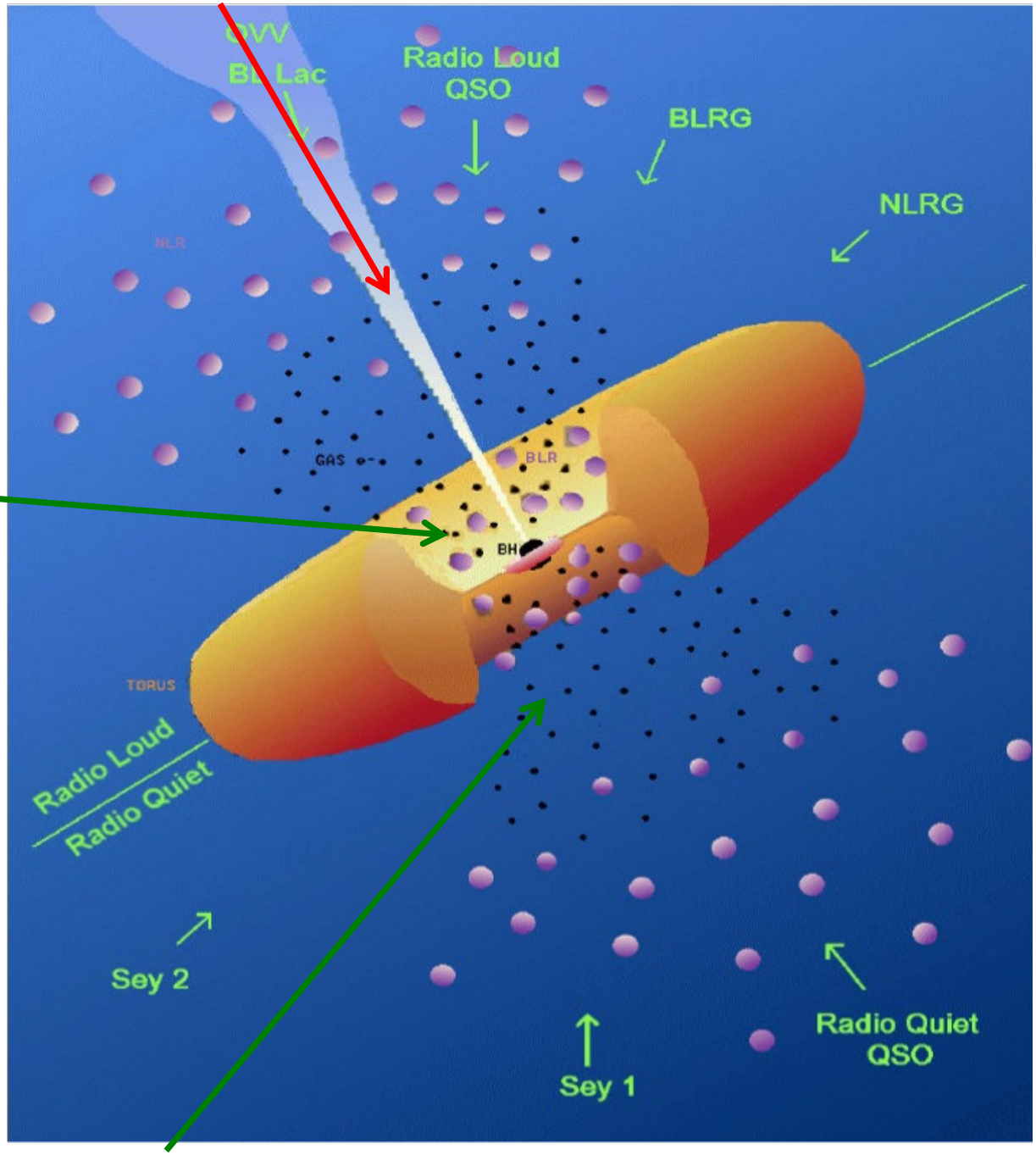

Broad line region

Narrow line region

- Schematic of geometry of active galactic nuclei. Adapted from Urry & Padovani (1995, PASP, **107**, 803).

IceCube Neutrinos from AGN

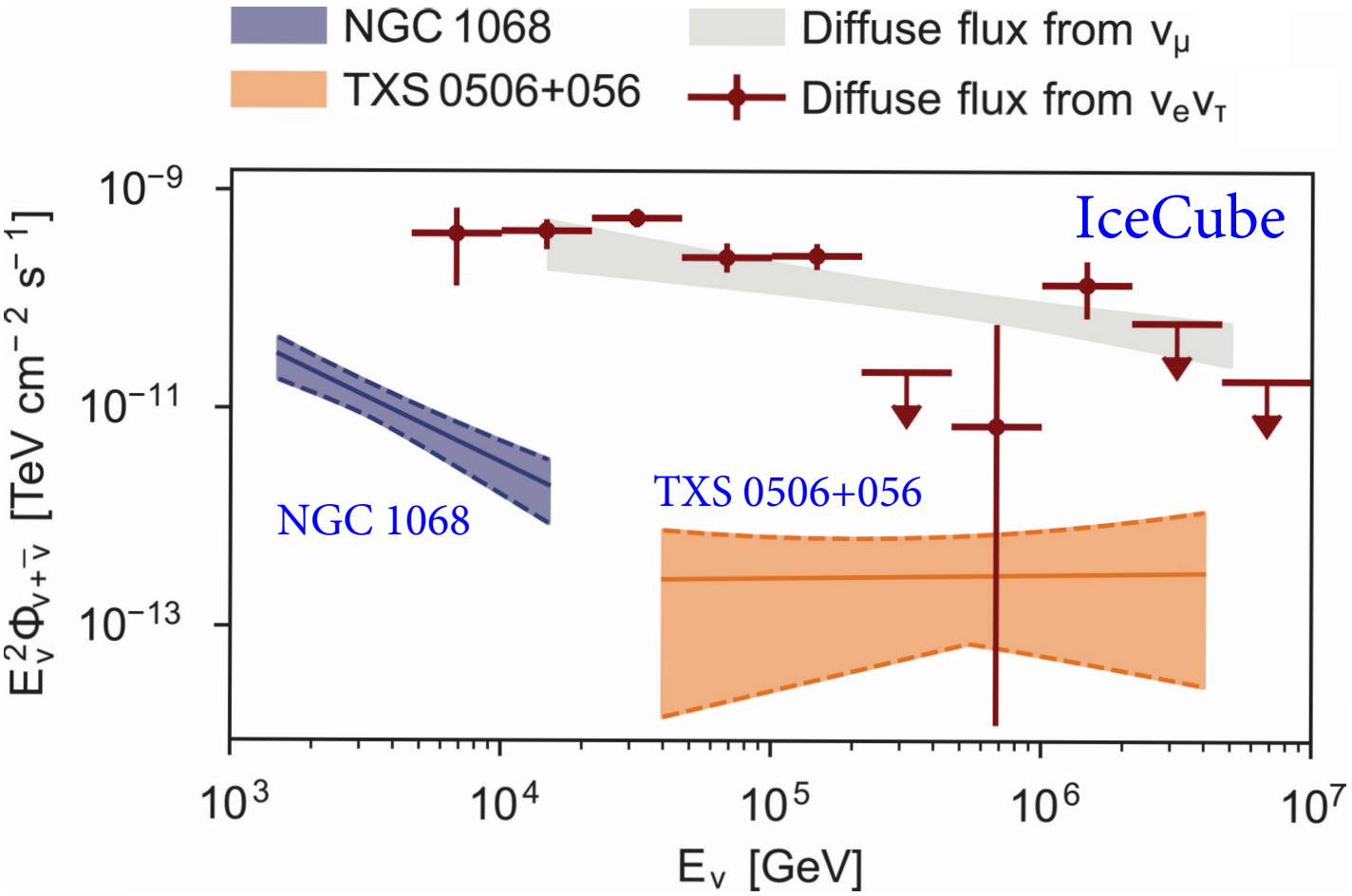

- IceCube neutrino spectra of the blazar TXS 0506+056 and the Seyfert II NGC 1068 compared with the diffuse neutrino signals.
- Abbasi et al. (Science **378**, 538, 2022).

5 Quasars

• Quasars were discovered in the early 1960s as **quasi-stellar objects** (QSOs) associated with radio sources. Their emission lines were broad, but coincided with no known atomic lines. M. Schmidt showed that these were redshifted Balmer lines for 3C 273, with $z = 0.158$. For quasars,

C & O, pp. 1095–9

$$z \;=\; \frac{\Delta\lambda}{\lambda_0} \;=\; \sqrt{\frac{1+v/c}{1-v/c}} \;-1 \quad , \quad z \;=\; 2 \;\;\Rightarrow\;\; v \;\approx\; 0.8c \qquad (16)$$

The emission lines are broad, with Doppler widths of $v \sim 10^4\,\mathrm{km/sec}$. Prominent emission lines are Lyman α, C IV and Mg II. High metallicity provides clues to active nucleosynthetic processing prior to the quasar phase. Epochs of prolific star formation at moderate to high z?

Combes Sec. 10.1

$*$ Appearance of both permitted (C IV at 1549Å; Mg II at 2798Å) and forbidden (OIII at 4959Å) is a signature of collisional excitation as well as ionization in the hot central quasar environs.

• There are also narrow absorption lines (metallic and otherwise), and these have moderate to high redshifts. This absorption implies intervening material at different redshifts along the line of sight, from other galaxies.

Plot: UV Spectrum of Quasar 3C 273 (z=0.158)

Quasar redshifts generally span $0.04 \lesssim z \lesssim 6.3$. They have strong absorption lines when $z \gtrsim 2$, but lower z (nearer) examples have little or no absorption. Their generally high redshifts imply that they possess large bolometric luminosities $L \sim 10^{45} - 10^{47}\,\mathrm{erg/sec}$.

Plot: Composite Quasar Spectra

• Quasars exhibit rapid optical and radio variability (polarized), on timescales of weeks and months, often have jets that are superluminal, and VLBI observations constrain the central engine to less than 10 light years in radius. Some quasars are also blazars, with one of their jets pointing more or less towards Earth.

Quasar 3C 273: UV-Blue Spectra

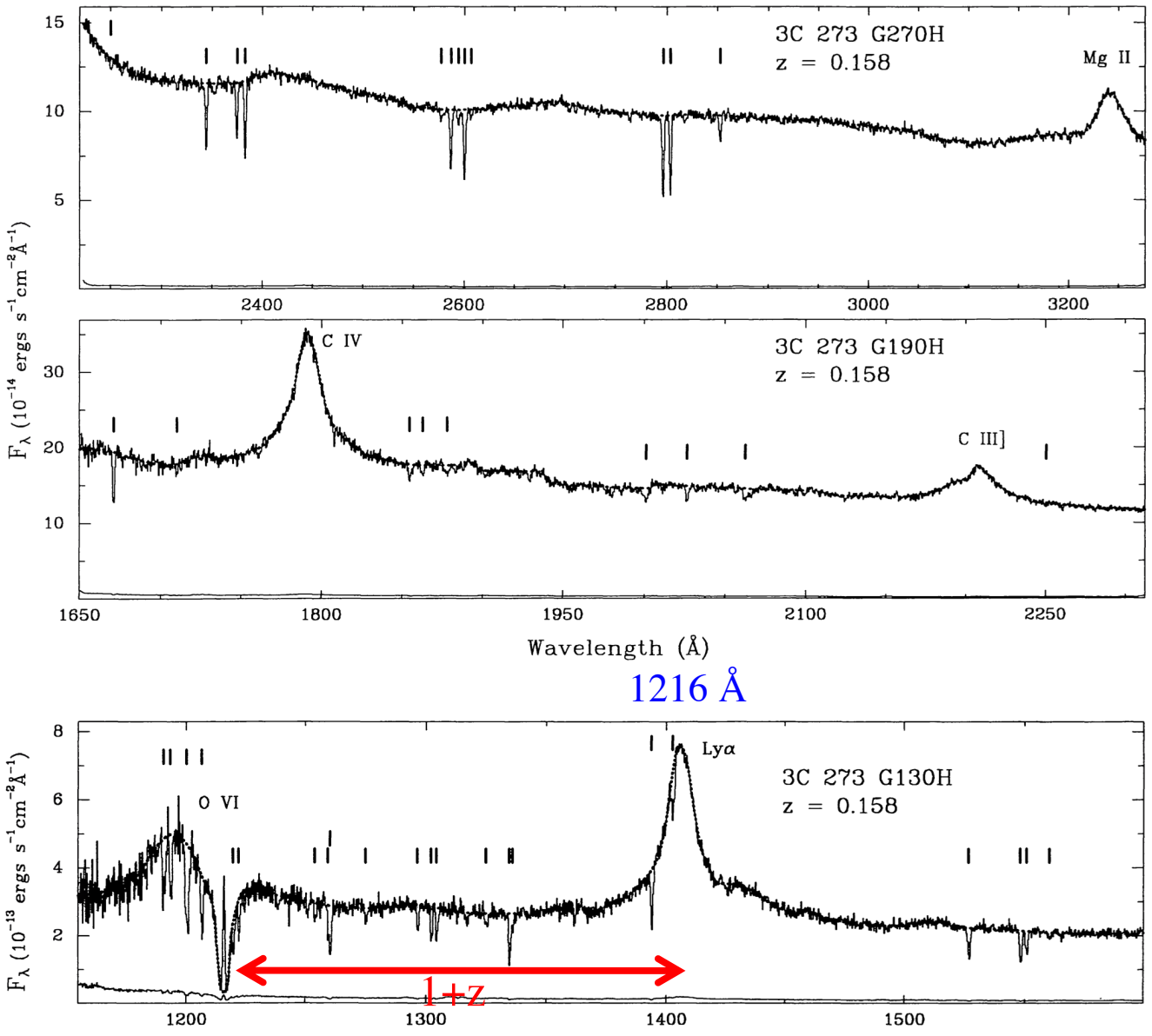

- From Bahcall et al. (1993, ApJS **87**, 1).

Composite Quasar UV-Yellow Spectra

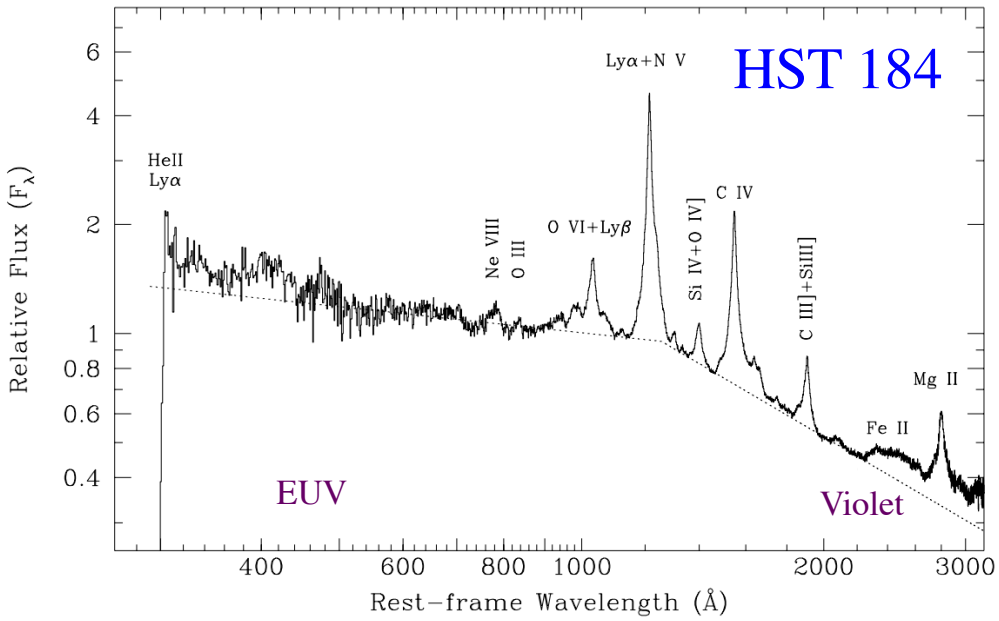

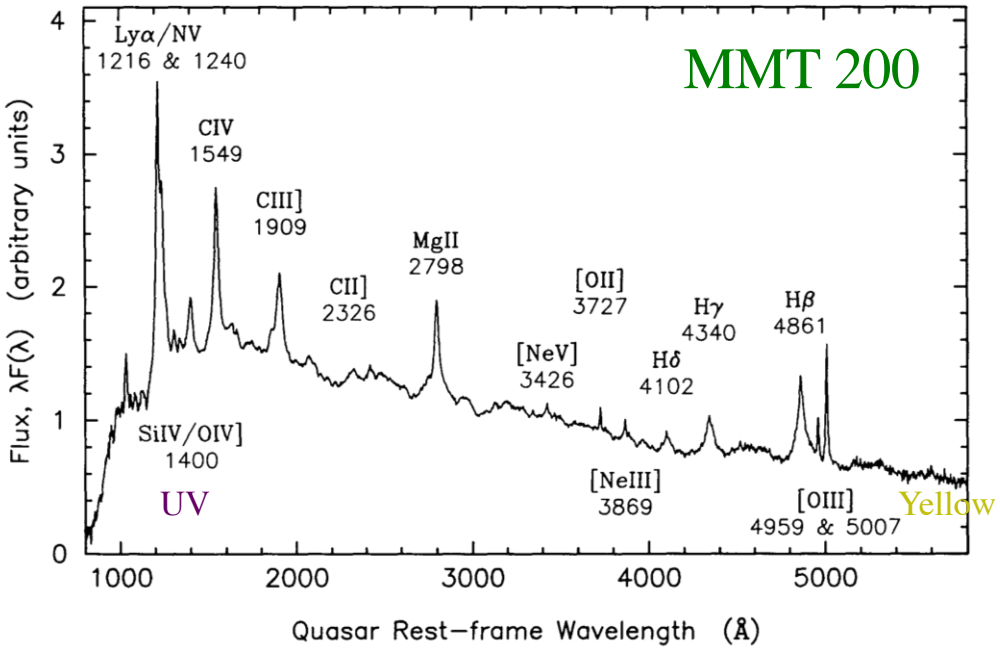

- *Left*: Composite of spectra from HST spectra from 184 quasars (z>0.33) in EUV-violet band. The co-adding is performed in the quasar rest frames so that lines appear at their natural wavelengths and redshifting is removed. From Telfer et al. (2002, ApJ **565**, 773).
- *Right*: Composite of MMT spectra from around 200 quasars in UV-yellow band from Francis et al. (1991, ApJ **373**, 465). Results differ somewhat from Telfer analysis because cosmological parameters were poorly known then, impacting de-redshifting protocols.

• The fact that quasars resemble radio galaxies in their radio morphology and spectra, and Seyferts in their emission lines suggests that quasars are perhaps an early evolutionary stage of the active galaxy zoo.

∗ There is growing evidence that quasars are indeed surrounded by "fuzz" that may be the parent galaxy.

• The Lyman alpha line L_α is at $\lambda_{L\alpha} = 1216$ Angstroms, so blueward of $\lambda_{L\alpha}/(1+z)$ no atomic hydrogen emission can appear, and a host of absorption lines is evident. This is called the **Lyman alpha forest**. **Longair Sec. 18.3**

Many different z are inferred from this forest $\Rightarrow$ a complex picture of locations of absorbing clouds along the line of sight. Diagnostics on the clouds are forged through **equivalent widths** W, defined via

$$W = \int \frac{I_{\rm cont} - I(\lambda)}{I_{\rm cont}}\, d\lambda \quad , \tag{17}$$

this being a measure of the fractional strength of the line relative to the mean continuum intensity $I_{\rm cont}$ bracketing a line. The line of sight **column density** n_H (in units of $\rm cm^{-2}$) is proportional to W.

∗ This protocol provides insights into the spatial distribution of baryonic matter in the fairly recent history of the Universe, providing a third dimension to complement sky maps and angular correlation functions of galaxies.

• High z quasars are subject to **gravitational lensing** by intervening galaxies, clusters and their dark matter. This phenomenon can be used to probe the dark matter distribution in the universe.